Biointerface Research in Applied Chemistry
Platinum Open Access Journal (ISSN: 2069-5837)

*Article*
**Volume 12, Issue 1, 2022, 809 - 823**
https://doi.org/10.33263/BRIAC121.809823

# Synthesis, Molecular Characterization, Biological and Computational Studies of New Molecule Contain 1,2,4-Triazole, and Coumarin Bearing 6,8-Dimethyl

**Pelin Koparir [1,*], Kamuran Sarac [2], Rebaz Anwar Omar [3,4,*]**

[1] Forensic Medicine Institute, Department of Chemistry, 44100 Malatya, Turkey; mpelin23@hotmail.com (P.K.);
[2] Bitlis Eren University, Faculty of Art and Sciences, Department of Chemistry, 13000 Bitlis, Turkey; ksarac@beu.edu.tr (K.S.);
[3] Department of Chemistry, Faculty of Science & Health, Koya University, Koya KOY45, Kurdistan Region – F.R. Iraq
[4] Fırat University, Faculty of Sciences, Department of Chemistry, 23000 Elazığ, Turkey; rebaz.anwar@koyauniversity.org (R.O.);
* Correspondence: mpelin23@hotmail.com (P.K.); rebaz.anwar@koyauniversity.org (R.O.);
Scopus Author ID 57222539130

**Received: 22.02.2021; Revised: 5.04.2021; Accepted: 9.04.2021; Published: 26.04.2021**

**Abstract:** Synthesis 4-(((4-ethyl-5-(thiophen-2-yl)-4H-1,2,4-triazol-3-yl)thio)methyl)-6,8-dimethyl-coumarin and spectral analysis is carried out using the FT-IR and NMR with the help of quantum chemical calculation by DFT/6-311(d,p). The molecular electrostatic potentials and frontier molecular orbitals of the title compound were carried out at the B3LYP/6-311G(d,p) level of theory. Antimicrobial, antioxidant activity, and *In vitro* cytotoxic for cell lines were observed. The result shows that the theoretical vibrational frequencies, 1H-NMR and 13C-NMR chemical shift, agree with experimental data. In vitro studies showed that antimicrobial activity was weak, particularly against bacteria such as *E. coli, S. aureus, P. aeruginosa,* and *B. cereus*. The test compound's oxidative stress index (OSI) has appeared as 0.079 ± 0.214 in antioxidant and oxidant capacity studies. The compound did not cause a harmful cytotoxic effect on healthy cell lines and showed no potential for anticancer activity on cancerous cell lines such as MCF-7 and MKN-45.

**Keywords:** coumarin; triazole; Gaussian; molecular modeling; cytotoxic; antioxidant.



## 1. Introduction

Natural products are an essential resource for drug development and design [1]. They have been used to treat diseases for thousands of years [2]. Benzene and coumarin derivatives containing pyrone rings are natural products found in high concentrations in fruits, seeds, leaves, and roots [3-7]. These structures can do hydrogen bonding, hydrophobic bonding, electrostatic interaction, metal coordination, and van der Waals force with proteins and enzymes [8, 9]. Thus, it can exhibit various biological activities such as antimicrobial, anti-inflammatory, antioxidant, and anticancer [10]. Because of their synthetic usefulness and a wide variety of biological activities, the chemistry of 1,2,4-triazoles has gained considerable attention [11]. Many research studies have shown that 1,2,4-triazoles have powerful biological characteristics, including antibacterial [12], antimicrobial [13], antifungal [14, 15], anticancer [16], antitubercular [17], antimycotic activity [18, 19], antinociceptive, [20], antioxidant [21, 22], anticonvulsants [23], antimycobacterial, antiviral [24], anti-inflammatory and analgesic [25].

Since coumarins have an effective biological activity, they have found wide use in medicinal chemistry. Today, it is known that the design and synthesis of new coumarin derivatives prepare new drugs in many laboratories.

In recent years, density functional theory (DFT) has become one of the commonly used theories in theoretical modeling. Through better functions of exchange-correlation, several molecular properties that have accuracy comparable to historically correlated ab initio methods can be measured, all of which could be achieved with more favorable computational costs [26, 27]. During the literature review, it was found that in the replication of the experimental values in geometry, dipole moment, vibrational frequency, etc., the exact precision of the DFT [28-32].

In this study, a new coumarin derivative 4 - (((4-Ethyl-5- (thiophen-2-yl) -4H-1,2,4-triazol-3-yl) thio) methyl) - 6,8-dimethyl-coumarin synthesized. Theoretical calculations were made after the structure of the title compound was determined. Also, biological effects such as antimicrobial, antioxidant, and cytotoxic were investigated.

## 2. Materials and Methods

### *2.1. Experimental.*

All chemical materials were received from Merck without 4-(chloromethyl)-7-methylcoumarin, which was received from an organic lab worker at Firat University. The Infrared spectra were measured with a Perkin–Emler Spectrum one FT-IR spectrophotometer. The $^{1}$H- and $^{13}$C-NMR spectra were recorded on Bruker AC-400 NMR spectrometer operating at 400 MHz for $^{1}$H-NMR, 100 MHz for $^{13}$C-NMR. Compounds were dissolved in DMSO (dimethyl sulfoxide), and chemical shifts were referenced to TMS (Tetramethylsilane) for both $^{1}$H- and $^{13}$C-NMR. Melting points were determined on the Thomas Hoover melting point apparatus. Chemicals were purchased from Aldrich or Merck.

#### 2.1.1. Synthesis of 4-Ethyl-5-(thiophene-2-yl)-4H-1,2,4-triazole-3-thiol (III).

A mixture of thiophene-2-carbohydrazide (I) (0.01 mol), ethyl alcohol (50ml), and ethyl isothiocyanate were refluxed for 3 h. After about 4 h, solid thiosemicarbazide begins to form in the reaction flask. KOH (0.15 mol) was added to the solid, and dissolution started. After 6 h, the reaction was stopped and brought to pH 3-4 with HCl. The residue was poured into crushed ice while stirring. The resulting solid was collected by filtration, dried, and recrystallized from ethyl alcohol.

FT-IR (KBr, cm$^{-1}$, υ): 3072-3107 (Ar-H), 2870-2960 (C-H), 1570 (C=N), 1263 (C=S), 715 (C-S-C); $^{1}$H NMR (400 MHz, DMSO-$d_6$, δ, ppm): 1.23 t (3H, N-$CH_2$-$CH_3$, *J* = 7.2 Hz), 4.22 q (2H, -N-$CH_2$-$CH_3$, *J* = 7.2 Hz), 7.27 dd (1H, Ar-H, *J* = 4.0, 4.8 Hz), 7.68 d (1H, Ar-H, *J* = 3.2 Hz) 7.86 d (1H, Ar-H, *J* = 4.8 Hz), 13.98 s (1H, SH); $^{13}$C-NMR (100 MHz, DMSO-$d_6$, δ, ppm): 13.7, 39.7, 126.8, 128.9, 129.3, 130.3, 146.3, 167.5.

#### 2.1.2. The synthesis of 4-(((4-ethyl-5-(thiophen-2-yl)-4H-1,2,4-triazol-3-yl)thio)methyl)-6,8-dimethyl-coumarin.

Potassium carbonate ($K_2CO_3$) (0.02 mol) was dissolved in 30 ml of dry acetone. The 4-(chloromethyl)-7-methylcoumarin (0.02 mol) was added to this solution. The 4-Ethyl-5-(thiophene-2-yl)-4H-1,2,4-triazole-3-thiol (III) (0.02 mol) was then added dropwise to this solution for 6 h at room temperature. The resulting solid was collected by filtration, dried, and

recrystallized from ethyl alcohol. Synthesis and the structure of the title compound are shown in Figure 1.

IR spectrum, υ, $cm^{-1}$ : 2940–3075 $cm^{-1}$ (Ar-H), 1720 (C=O), 1617-1327 $cm^{-1}$ (C=C), 1346-1469 $cm^{-1}$ 522-831 (C-S); $^{1}$H-NMR (400 MHz, DMSO-$d_6$, δ, ppm): 1.16 (t, 3H, N-$CH_2$-$CH_3$, *J* = 7.0 Hz), 2.51 s (3H, Ar-$CH_3$, ), 3.18 s ( 3H, Ar-$CH_3$), 4.09 q (2H, N-$CH_2$-$CH_3$, *J* =6.9 Hz), 4.61 s (2H, S-$CH_2$), 6.35 (s,1H, H-C-C=O), 7.22 s (1H, Ar-H), 7.26 dd (1H, thiophene-H), 7.55 d (1H, thiophene-H), 7.63 s (1H, Ar-H), 7.80 d (1H, thiophene-H) ; $^{13}$C-NMR (100 MHz, DMSO-$d_6$, δ, ppm):15.28, 19.04 20.05, 33.62, 114.3, 115.7, 117.8, 125.6, 127.5, 128.1, 128.7, 129.4, 133.6, 149.2, 150.1, 151.2, 151.9, 160.2.

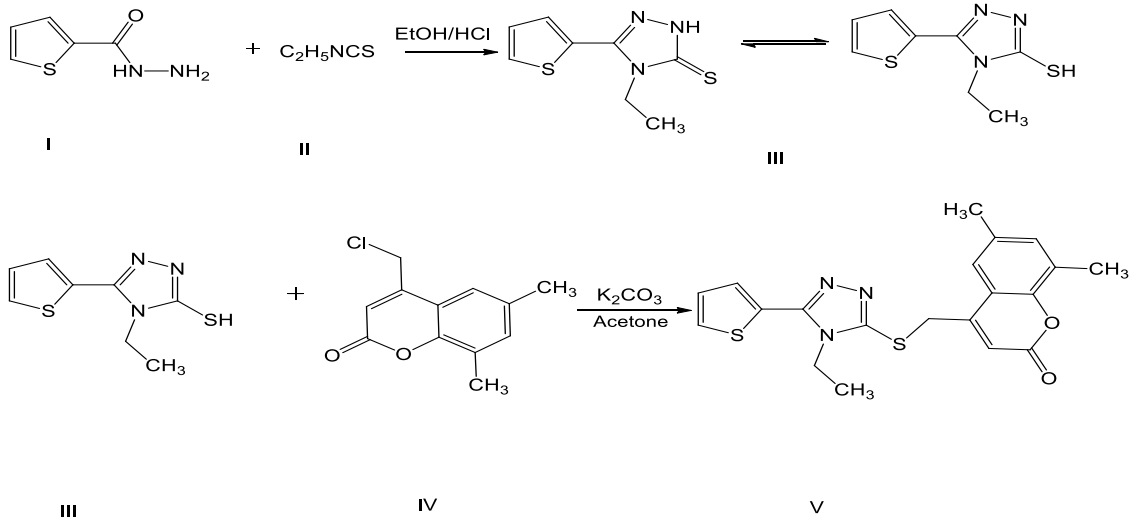


**Figure 1.** Synthesis of the title compound.

*2.2. Computational methods.*

All theoretical calculations (optimizations, NMR and IR ) in this study were computed via Gaussian 09 software [33]. Visualizing of results was made using the GausView5 program. In theoretical computations, the DFT/B3LYP method and 6-311G (d,p) were selected as the basis set [34]. Theoretical NMR shifts ($^{1}$H-NMR and $^{13}$C-NMR) were computed within the GIAO approach [35]. In NMR calculations, DMSO was selected DMSO as solvent. Experimental infrared frequencies are different from computed infrared frequencies.

*2.3. Biological methods.*

2.3.1. Antimicrobial activity detection.

The antimicrobial activity of the test compound was determined by the "Microdilution Broth Method" by determining the minimum inhibition concentration (MIC) of plant extracts against microorganisms [36, 37]. Microorganism strains used in the study; *Staphylococcus aureus* (ATCC 29213), *Pseudomonas aeruginosa* (ATCC 27853), *Escherichia coli* (ATCC 25922), *Bacillus cereus* (ATCC 11778), *Candida albicans* (ATCC 10231), and *Candida tropicalis* (DSM 11953). The stock solution was prepared by dissolving the test title compound in 40% Dimethyl sulfoxide (DMSO). Mueller Hinton Broth (Accumix® AM1072) for bacterial strains, Saboraud Dextrose Broth (Himedia ME033) for *Candida albicans*, and *Candida tropicalis* were used. A sterile Pasteur pipette added 90 µl (MHB for antibacterial, SDB for antifungal) to the wells in the first row of microliter plates and 50 µL each to the other wells.

The 11 wells row were used as a sterility control, and 100 µL of the medium was added to each (CLSI, 2002; CLSI, 2012). The wells in the 12th row were used as growth control. 10 µL of the stock solution of the test compound was added to the first wells, and the other wells were added by serial dilution. A suspension equivalent to McFarland 0.5 solution was prepared from microorganisms. 50 µL of microorganism suspension was added to each well at 5 x 105 CFU / mL for bacteria and 0.5-2.5 x103 CFU / mL for *Candida albicans* and *Candida tropicalis.* Plates with bacteria added were incubated at 37 ° C, plates with Candida albicans and *Candida tropicalis* added at 35 ° C for 16-24 hours. In the evaluation of the results, the first wells in which the turbidity or appearance of the microorganisms decreased was accepted as the MIC value. The test was repeated 3 times.

2.3.2. Determination of total antioxidant and total oxidant levels.

The total antioxidant level (TAS), total oxidant level (TOS), and oxidative stress index (OSI) of the test compound was determined using commercially available Rel Assay Diagnostic kits with the formulas given below. Trolox standard for TAS analysis, hydrogen peroxide standard for TOS analysis used as reference. Oxidative stress index (OSI (Arbitrary Unit = AU) value is calculated according to the formula below [38].

$$OSI\ (AU) = \frac{\text{TOS, µmol H2O2 equiv./L}}{\text{TAS, mmol Trolox equiv./L X 10}}$$

2.3.3. Cell cultures study.

In the study, Breast cancer cell lines (MCF-7), Human gastric cancer cell lines (MKN-45), and Human umbilical vein endothelial cells (HUVECs) are used.

2.3.4. Process of growing and reproducing cells.

All cell lines are collected in 25 $cm^2$ flasks (Corning-Sigma-Aldrich St. Louis, MO, USA) in an incubator at 37°C with 5% $CO_2$ content, Dulbecco's modified Eagle's medium (containing high glucose, 2mM L-glutamine and sodium pyruvate). DMEM) and 10% Fetal Bovine Serum (FBS). When the cell's growth and morphologies were followed, reached 90% density, the transplantation process was started (Nuve MN 120). The 200 µL of the mixture was put into each of 96 wells (5x103 cells in 100 µl / plate space). DMEM, fetal bovine serum (FBS), and sterile phosphate buffer (PBS) were purchased commercially.

2.3.5. MTT experiment.

MTT assay method was used to determine the effects of the test compound in cell cultures. The MTT test (3- [4,5-dimethyl thiazol-2-y 1] -2,5-diphenyl tetrazolium bromide) is a colorimetric analysis method used to evaluate the metabolic activity of the cell. Test compound at different concentrations (1-10-100-1000 mg / mL) was added to the 96-well plates where the cells were cultivated, following the cells' adhesion. After 24 hours, 10 µL of 12 mM MTT solution was added to the wells and incubated for 4 hours at 37 ° C in an oven containing 5% $CO_2$.

The purple-colored formazan crystals formed after 4 hours, 100 µL of SDS dissolved in 0.01M HCl was added and left for incubation at 37 °C in an oven containing 5% $CO_2$. The absorbance of the purple color formed after 4 hours was measured with an Elisa plate at 570

nm. IC50 values of the test compound were calculated according to MTT results obtained using Graphpad prism 6 programs on the computer.

2.3.6. Statistical analysis.

SPSS 22.0 (IBM Corporation, Armonk, New York, United States) program was used to analyze the data. The data were analyzed at 95% confidence level, and if the p-value was less than 0.05, it was considered significant.

## 3. Results and Discussion

*3.1. Molecular geometry.*

Figure. 2 presents the theoretical geometric structure and the B3LYP/6-311G(d,p) optimized structure of the title compound.

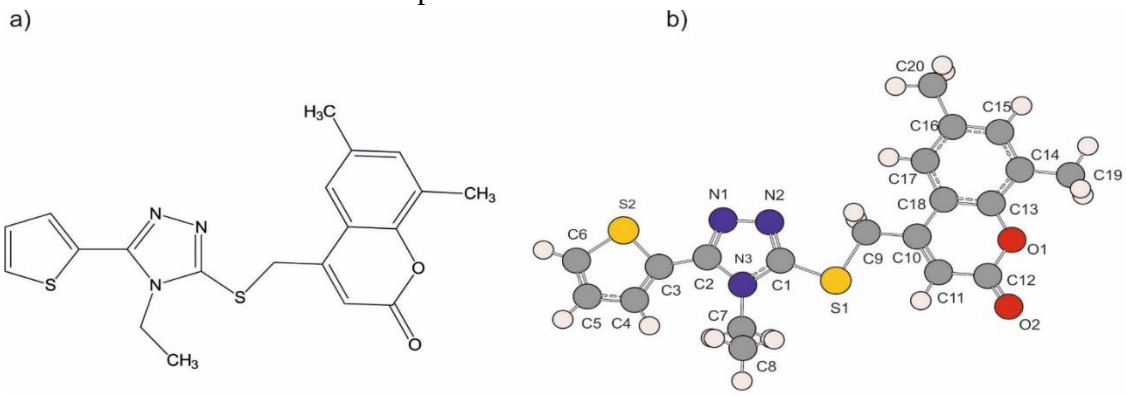


**Figure 2.** (a) The experimental geometric structure of the title compound. (b) The theoretical geometric structure of the title compound with B3LYP/6-311G(d,p) level.

*3.2. Nuclear magnetic resonance (NMR) spectra.*

B3LYP method with 6-311G(d,p) basis set was used to calculate GIAO $^{1}H$ and $^{13}C$ chemical shift values (concerning TMS), which then compared with the experimental $^{1}H$ and $^{13}C$ chemical shift values shows the results Table 1. When the experimental and theoretical $^{1}H$-NMR and $^{13}C$-NMR spectra of the compound are examined, there are some characteristic peaks in the substituents attached to the triazole and coumarin ring.

The first example of these substituents is the ethyl fragment. While the -$CH_2$ protons of the N-$CH_2$-$CH_3$ in the 3-position were observed to give a quartet peak at 4.09 ppm (*J* value of this quartet peak is around 6.9 Hz), the same protons were computed as at 4.14 ppm. While the -$CH_3$ protons showed triplet at 1.16 ppm (The *J* value of this triplet peak is 7.0 Hz), the same protons were calculated at 1.30 ppm. The carbons in the $^{13}C$-NMR spectrum of the ethyl group were observed at 15.3 ppm for $CH_3$, at 33.6 ppm for $CH_2$ as experimental, and the same carbons were computed at 16.2 ppm and 35.9 ppm, respectively. Because of the high electronegativity of the nitrogen atom, carbon and hydrogen atoms close to the nitrogen atom are set downfield. Thus, the electron charge density shifts from these atoms toward the nitrogen atom, and these atoms resonance downfield.

The second example of these substituents is the S-$CH_2$ fragment. The protons in the fragment -S-$CH_2$- were appeared as a signal singlet at 4.61 ppm experimentally. These protons were calculated at 4.44 ppm at the B3LYP level. The carbon belonging to the S-CH2 group in the $^{13}C$-NMR spectrum appeared at 40.1 ppm experimentally, and the same carbon was

computed at 41.9 ppm. The reason why the carbon and hydrogens attached to the sulfur atom are observed in the low field is the electronegativity of the sulfur atom. Electrons around the proton and carbon atom shift towards the sulfur atom, and thus a low electron density occurs around these atoms, which reduces the shielding effect of carbon and hydrogen, and these atoms resonance in downfield.

The final example of these substituents is $CH_3$ fragments in the coumarin ring. Methyl is attached to the coumarin ring at both the C14 and C16 positions has an electron-donating structure [39]. As this structure donates electrons to the ring, it increases the electron density of the ring, which means that the protons bound to C15 and C17 in the aromatic ring resonance at a higher field and chemical shift values were observed as a singlet at 7.22 and 7.63 ppm experimentally, and as computed at 7.05 and 7.63 ppm, respectively. Chemical structure, $^{1}$H- and $^{13}$C-NMR spectra of the title compounds are shown in Figures 3–4.

**Table 1.** Experimental and Calculated Chemical Shifts (Ppm) Of $^{1}$H-NMR and $^{13}$C-NMR for The Title Compound (V).

| **Atom** | **Experimental (ppm) DMSO-$d_6$** | **Theoretical (ppm9) B3LYP/6-311G(d,p)** |
|---|---|---|
| C1 | 149.2 | 157.5 |
| C2 | 151.9 | 158.1 |
| C3 | 149.1 | 141.9 |
| C4 | 129.4 | 131.6 |
| C5 | 128.1 | 132.7 |
| C6 | 128.7 | 139.1 |
| C7 | 33.6 | 35.9 |
| C8 | 15.3 | 16.2 |
| C9 | 40.1 | 41.9 |
| C10 | 151.2 | 155.8 |
| C11 | 114.3 | 115.8 |
| C12 | 160.2 | 165.1 |
| C13 | 150.1 | 159.2 |
| C14 | 125.6 | 123.2 |
| C15 | 127.5 | 130.3 |
| C16 | 133.6 | 131.3 |
| C17 | 117.8 | 120.5 |
| C18 | 115.7 | 121.1 |
| C19 | 19.1 | 22.3 |
| C20 | 20.1 | 24.1 |
| 3H (thiophene-H) | 7.80, 7.55 and 7.26 | 7.56, 7.44 and7.33 |
| 2H (N-CH2-CH3) | 4.09 | 4.14* |
| 3H (N-CH2-CH3) | 1.16 | 1.30* |
| 2H (S-CH2) | 4.61 | 4.44* |
| 1H (H-C-C=O) | 6.35 | 6.25 |
| 6H (Ar-CH3) | 2.51 and 3.18 | 2.16* and 2.35* |
| 2H (Ar-H) | 7.22 and 7.63 | 7.05 and 7.36 |

*: Average values

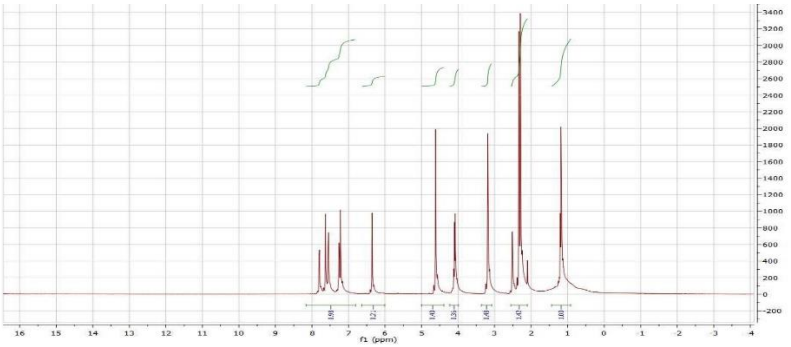

**Figure 3.** $^{1}$H-NMR spectrum for the title compound (V).

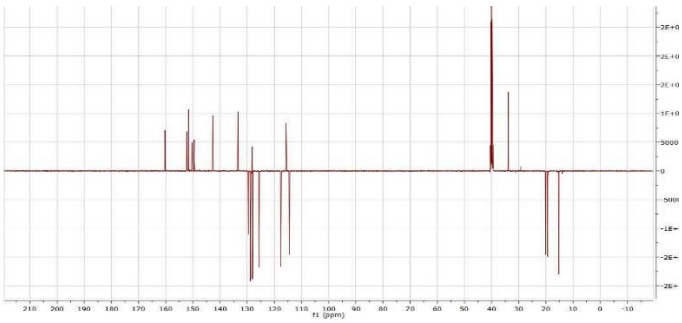

**Figure 4.** $^{13}$C-NMR spectrum for the title compound (V).

*3.3. Fourier-transform infrared spectroscopy (FT-IR).*

In the first step of this work, When the FT-IR spectra of the synthesized 4-Ethyl-5-(thiophene-2-yl)-4H-1,2,4-triazole-3-thiol (III) were examined, it was found that the C=O peak in the carboxylic acid hydrazides between 1640-1670 $cm^{-1}$ was disappeared. Instead of this peak, N-C=S peaks (amide bands) at 1574, 1267, 1065, and 995 $cm^{-1}$ appeared. In the title compound (V) obtained in the second step of the work, the most characteristic peaks are CO, CH, and CH3 vibrations.

3.3.1. CO vibrations.

The title Compound was observed at two types of CO stretching vibrations; the first one was C–O (O1-C12 and C13-O1), and the second one was C=O (C12=O2) stretching vibrations. The C-O stretching frequency was shown in the range of 1250-850 $cm^{-1}$ [40]. The title compound C-O stretching vibrations (O1-C12 and C13-O1) appeared at 940 cm-1 and 1270 cm-1 experimentally and calculated at 915 cm-1 and 1240 cm-1 B3LYP/6-311G(d,p) level, respectively. The C=O stretching vibrations were observed in the range of 1650-1850 $cm^{-1}$. The title compound C=O stretching vibration was appeared at 1720 $cm^{-1}$ experimentally and calculated at 1755 $cm^{-1}$ for B3LYP/6-311G(d,p) level. The appearance of C-O and C=O stretching vibrations in the title compound is an important indicator of the presence of the coumarin ring.

3.3.2. CH and CH3 vibrations.

CH stretching vibrations in the aromatic ring are seen in the frequency range of 3100-3000 $cm^{-1}$ (in the form of multiple bands) [41]. The title compound CH stretching vibrations were appeared between 2937-3081 $cm^{-1}$ experimentally and calculated at 2983-3144 $cm^{-1}$ for B3LYP/6-311G(d,p) level. CH stressing vibrations are mostly observed in-plane bending (scissoring and rocking) and out-of-plane bending (wagging and twisting) vibrations. In-plane bending vibrations are seen between 1400-1050 $cm^{-1}$, and out-of-plane bending vibrations are seen between 1000-675 $cm^{-1}$ [42-44]. In the synthesized title compound, the in-plane bending vibrations were shown in 1350-1045 $cm^{-1}$ experimentally and calculated 1341-1028 $cm^{-1}$ for B3LYP. The out-of-plane bending vibrations were appeared in 850-723 $cm^{-1}$ experimentally and calculated 828-695 $cm^{-1}$ for B3LYP.

CH3 stretching (symmetrical and asymmetrical) vibrations are seen in the frequency range of 2850-3000 $cm^{-1}$ [45, 46]. CH3 stretching vibrations in title compound appeared at 2937 $cm^{-1}$ (Vs, triazole), 3051 (Vs coumarin, C19), 3009 $cm^{-1}$ (Vs coumarin, C20) experimentally, and calculated 2928 $cm^{-1}$ (Vs, triazole), 3020 (Vs coumarin, C19), 2981 $cm^{-1}$

(Vs coumarin, C20) respectively. Some other important peaks as C=C, C-S and C=N vibrations are seen in the frequency range of 1650-1200 $cm^{-1}$, 600-772 $cm^{-1}$, 1675-1480 $cm^{-1}$, respectively according to the literature [47], while for our compound obtained between 1655–1340 $cm^{-1}$, 550-760 $cm^{-1}$, 1472-1429 $cm^{-1}$ , experimentally, respectively and calculated between 1617–1327 $cm^{-1}$, 522-831 $cm^{-1}$, 1346-1469 $cm^{-1}$, respectively. Also, Table 2 is shown at other levels of calculations.

According to these results, it is seen that there are some differences between experimental and theoretical calculated values. The first reason for these differences is that the experimental results were taken in the solid phase and the gas phase's theoretical results.

Secondly, in Gaussian infrared calculations belong to harmonic frequencies. However, in reality, there are anharmonic oscillations in molecules. Finally, experimental calculations are found in the presence of intermolecular interactions, but theoretical calculations are made on a single molecule.

**Table 2**. The Observed and Calculated Vibrational Spectra of the Title Compound.

| Assignments | Unscaled Frequencies (B3LYP/6-311(d,p) | Experimental (FT-IR(cm-1)) |
|---|---|---|
| υsC17H | 3090 | |
| υasC15H | 3060 | |
| υC11H | 3110 | |
| υsC6H | 3147 | |
| υasC5H | 3107 | |
| υsC4H | 3128 | |
| υC19H | 3022 | 3051 |
| υC20H | 2981 | 3009 |
| υC9H | 3019 | |
| υsC7H | 3028,2968,3007 | |
| υsC8H | 3028,2928,3007 | 2937 |
| υC12O2 | 1755 | 1720 |
| υC10C11 | 1617,1567 | 1655 |
| υN2C1 | 1346,1415 | 1429 |
| υN1C2 | 1469,1415 | 1472 |
| υC5C6 | 1472,1415,1327 | |
| υC3C4 | 1552,1415,1327 | 1340 |
| υC1N3 | 1371,1346 | |
| υC13O1 | 1240,1095 | 1270 |
| υC12O1 | 1134,915 | 940 |
| υN1N2 | 1064 | 1084 |
| υN3C7 | 1203,676 | |
| υS2C6 | 831,726 | 760 |
| υS1C1 | 546,522 | 550 |
| υS1C9 | 762,607 | |
| βC9C10C11 | 1363,1134,806 | 1348 |
| βN3C1N2 | 1415,1203 | 1392 |
| βC13C14C15 | 1240 | |
| βS2C6H | 1327,1116 | |
| βS1C9H | 1159,906 | |
| βO1C12O2 | 806, 573,568 | |
| βO1C13C14 | 915 | |
| βN2N1C2 | 1337,922 | |
| ωC15H | 1341 | 1350 |
| ωC5H | 1077 | 1084 |
| ωC19H | 1028 | 1045 |
| αC10C18C17H | 886,857 | |
| αO1C12C11H | 910,857,828 | 897 |
| αC1S1C9H | 1226,1159,910 | |
| αN3C7C8H | 1457,1121,1068 | |
| αN3C1N1N2 | 704,664 | |
| αS2C6C5C4 | 883,546 | |
| δO2C11O1C12 | 828,695 | 850 |
| δC3N3N1C2 | 704 | 723 |

υ, stretching; β: bending; ω: in-plane bending; δ: out of plane bending; α: torsional; s: symmetric; as asymmetric.

As a result, although there are some differences between experimental and theoretical values, it is seen that the results are in great agreement.

*3.4. Frontier molecular orbitals and global reactivity descriptors.*

Frontier molecular orbital theory applies Molecular orbital theory describing HOMO - LUMO interactions [48-50]. Global reactivity descriptors are given softness, hardness, and electronegativity in the literature [51-53]. As seen in Figure 5 the HOMO-1 electrons are delocalized on the coumarin ring; the HOMO electrons are delocalized on the triazole and thiophene ring, the LUMO electrons are delocalized coumarin ring, the LUMO+1 electrons are delocalized on the triazole and thiophene ring. The value of the energy separation between the HOMO and LUMO is 4.068 eV. This shows that the energy gap reflects the chemical activity of the molecule. For a molecule, by using HOMO and LUMO energy values can calculate the following parameters:

Ionization potential is the minimum amount of energy required to remove an electron from the atom or molecule in the gaseous state. Electron affinity is defined as the amount of energy released when an electron is added to a molecule in the gaseous state. Electronegativity is the tendency of an atom to attract electrons. Chemical hardness is a measure of the prevention of weight transfer in molecules. The molecules with higher chemical hardness values have little or no weight transfer [54]. Electronic structure parameter values calculated by the B3LYP method using 6-311G(d,p) are showed in Table 3.

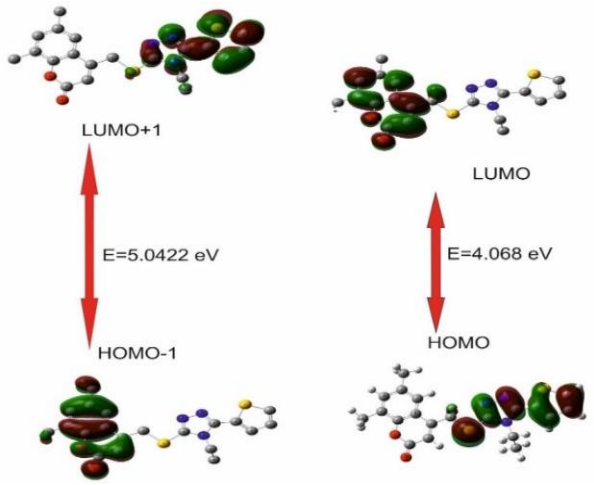


**Figure 5.** Energy levels of HOMO, HOMO-1, LUMO and LUMO-1 of the title compound (V) computed at B3LYP/6-311 G(d,p) level.

**Table 3.** Global Reactivity Descriptors for the Title Compound (V).

| Parameters | Gas phase |
|---|---|
| $E_{HOMO}$ | -6.040 |
| $E_{LUMO}$ | -1.972 |
| $\chi$ | 4.006 |
| $\eta$ | 2.034 |
| S | 0.245 |
| E=HOMO-LUMO | 4.068 |

Consideration of only the HOMO and LUMO may not yield a realistic description of the frontier orbitals because in the boundary region, neighboring orbitals may show quasi degenerate energy levels. For this reason, the density of states (DOS) was calculated both the gas phase by using the Gauss Sum 3.0 software [55]. Figure 6 is shown the density of states diagram for the title compound.

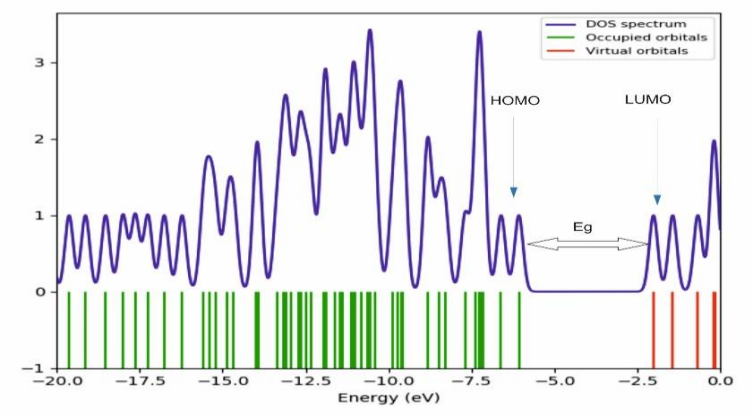


**Figure 6.** The density of states diagrams for the title compound (V).

*3.5. Molecular electrostatic potential (MEP).*

Molecular Electrostatic Potential [56] is related to dipole moment, electronegativity, partial charges, and the molecule's chemical reactivity region. It provides a visual method to understand the relative polarity of the molecule. While the negative electrostatic potential is the region where the electron density is higher than the nucleus over the entire molecule (colored in red tones on the ESP surface), the positive electrostatic potential is the region where the low electron density is high. (Colored in blue tones on the ESP surface) [57,58]. The MEP map of the compound is given in Figure 7.

According to the figure, the negative regions in the molecule are located on the Nitrogen N1 (−0.018 a.u.), N2 (−0.013 a.u.) atoms of the triazole ring, and Oxygen O1 (−0.021 a.u.), O2 (−0.041 a.u.) atoms of the coumarin ring. It can be said that these regions are the most suitable regions for the electrophilic attack. For the positive regions, it is seen that the ethyl group attached to the triazole ring with a value of (+0.027 a.u.) is located around the hydrogens, which can be said to be the region most susceptible to nucleophilic attack.

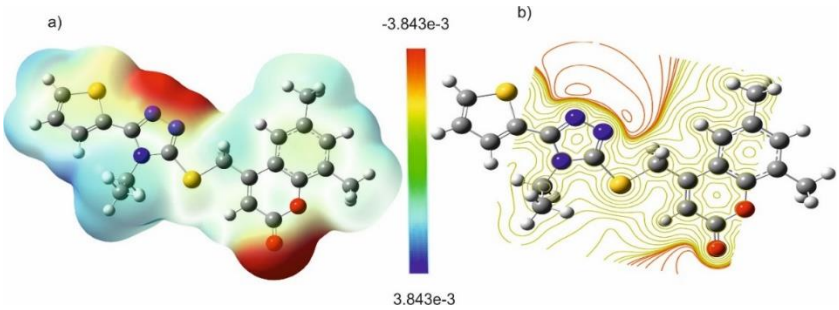


**Figure 7.** (a) Molecular electrostatic potential map calculated at B3LYP/6-311G(d,p) level. (b) Contour shape of the title compound.

*3.6. Antimicrobial activity.*

The antimicrobial activity of the test compound dissolved in DMSO is shown in Table 4. The test title compound is known to be significant when the MIC value is 0.1 mg / mL or less, moderately effective in the range 0.1 <MIC ≤ 0.625 mg / mL, and weakly effective when greater than 0.625 mg / mL [59]. In this study, it is seen that, in general, the test compound has moderate antimicrobial activities on some of the 6 different microorganism strains tested. The test title compound does not have a strong effect on the microorganisms tested. In general, it can be said that the test title compound is more effective on *B. cereus*, *P. aeruginosa*, and fungi.

**Table 4.** Antimicrobial Activities of the title Compound (Mg/Ml).

| | *E. coli* | *S. aureus* | *P. aeruginosa* | *B. cereus* | *C. albicans* | *C. tropicalis* |
|---|---|---|---|---|---|---|
| | ATCC 25922 | ATCC 29213 | ATCC 27853 | ATCC11778 | ATCC10231 | DSM11953 |
| The title compound | >5 | 2.5 | 2.5 | 2.5 | 2.5 | 1.25 |

*3.7. Antioxidant activity.*

The antioxidant potential of the active ingredient or compounds is generally due to their ability to remove or transform the effects of damaging free radicals. The higher antioxidant capacity of the compounds, the better the therapeutic quality [60]. In this study, the antioxidant capacity, oxidant capacity, and oxidative stress indices of the compound are given in Table 5. The title compounds may contain both oxidizing groups and oxidation-inhibiting groups, so it is important to calculate the total oxidative stress index and evaluate the overall antioxidant-oxidant load. According to the experiment results, the antioxidant value of the synthesized compound is 6.198 ± 0.310. When the oxidant load was examined, it was found to be 4.903 ± 0.122. When the oxidative stress index is examined, it is seen that it is 0.079 ± 0.214.

**Table 5.** TAS, TOS and OSI values of the compound.

| | **TAS (mmol/L)** | **TOS (µmol/L)** | **OSI** |
|---|---|---|---|
| The title compound | 6.198±0.310 | 4.903±0.122 | 0.079±0.214 |

*3.8. In vitro cytotoxic activity.*

Doses of the test compound at varying concentrations of 1, 10, 100, and 1000 µg / mL were administered on three different cell lines and left to incubation for 24 hours. IC50 value showing the test compound's cytotoxic effects on different cell lines is given in Table 6. It has been determined that IC50 values are generally well above the 10 µM dose. Therefore, it can be said that the test compound does not have a significant cytotoxic effect on the cell lines tested. The very weak cytotoxic effect of the test compound on the HUVEC cell line is beneficial for the compound's anticarcinogenic potential. It indicates that the synthesized test compound has no detrimental cytotoxic effect on healthy cells, shown in Table 6. However, the lack of a strong cytotoxic effect of the synthesized test compound on cancerous cell lines such as MCF-7 and MKN-45 indicates that the synthesized compound does not have a drug potential to be effective on these types of cancer.

**Table 6.** Ic50 Values indicating the Cytotoxic Effects of the Compound in Different Cell Lines.

| | **MCF7 Human breast adenocarcinoma cell line** | **HUVEC Human umbilical vein endothelial cell line** | **MKN-45 Human gastric cancer cell line** |
|---|---|---|---|
| The title compound | 981,198 | 978,561 | 196,475 |

## 4. Conclusions

In this study successfully Synthesis 4-((4-ethyl-5- (thiophen-2-yl) -4H-1,2,4-triazol-3-yl thio) methyl) -6,8-dimethyl-coumarin by the reaction of 6, 8-(dimethyl) -4- (chloromethyl) –coumarin and 4-ethyl-5- (thiophen-2-yl) -4H-1,2,4-triazole-3-thiol. Characterization of 6-ethoxy-4-methylcoumarin was confirmed by FT–IR, $^{1}$H NMR, and $^{13}$C NMR. The spectroscopic and electronic properties of the title compound were investigated both experimentally and theoretically. The title compound's structural data (V) calculated at B3LYP/G-311G(d,p) were in very good correspondence with experimental values. HOMO-LUMO boundry orbitals of the title compound, the energy difference between them, were

calculated. Also, it was determined in which regions the substituents in the compound were localized and whether the molecule had a stable structure. The regions closest to the electrophilic and nucleophilic attack were determined by creating a Molecular Electrostatic Potential (MEP) map. An agreement was determined between the theoretical and experimental results concerning the accurate allocation of the vibrational frequencies to the molecular structure based on the theoretical calculations. The antioxidant, antimicrobial and cytotoxic properties of the title compound were studied.

## Funding

This research received no external funding.

## Acknowledgments

This research has no acknowledgment.

## Conflicts of Interest

The authors declare no conflict of interest.

## References

1. Lee, A.C.-L.; Harris, J.L.; Khanna, K.K.; Hong, J.-H. A comprehensive review on current advances in peptide drug development and design. *International journal of molecular sciences* **2019**, *20*, https://doi.org/10.3390/ijms20102383.
2. Li, W.; Sun, Y.N.; Yan, X.T.; Yang, S.Y.; Kim, E.-J.; Kang, H.K.; Kim, Y.H. Coumarins and lignans from Zanthoxylum schinifolium and their anticancer activities. *Journal of agricultural and food chemistry* **2013**, *61*, 10730-10740, https://doi.org/10.1021/jf403479c.
3. Borges, F.; Roleira, F.; Milhazes, N.; Santana, L.; Uriarte, E. Simple coumarins and analogues in medicinal chemistry: occurrence, synthesis and biological activity. *Current medicinal chemistry* **2005**, *12*, 887-916, https://doi.org/10.2174/0929867053507315.
4. Borges Bubols, G.; da Rocha Vianna, D.; Medina-Remon, A.; von Poser, G.; Maria Lamuela-Raventos, R.; Lucia Eifler-Lima, V.; Cristina Garcia, S. The antioxidant activity of coumarins and flavonoids. *Mini reviews in medicinal chemistry* **2013**, *13*, 318-334, https://doi.org/10.2174/13895713804999775.
5. Davis, R.A.; Vullo, D.; Maresca, A.; Supuran, C.T.; Poulsen, S.-A. Natural product coumarins that inhibit human carbonic anhydrases. *Bioorganic & medicinal chemistry* **2013**, *21*, 1539-1543, https://doi.org/10.1016/j.bmc.2012.07.021.
6. Zhang, L.; Jiang, G.; Yao, F.; He, Y.; Liang, G.; Zhang, Y.; Hu, B.; Wu, Y.; Li, Y.; Liu, H. Growth inhibition and apoptosis induced by osthole, a natural coumarin, in hepatocellular carcinoma. *PloS one* **2012**, *7*, https://doi.org/10.1371/journal.pone.0037865.
7. Lončar, M.; Jakovljević, M.; Šubarić, D.; Pavlić, M.; Buzjak Služek, V.; Cindrić, I.; Molnar, M. Coumarins in Food and Methods of Their Determination. *Foods* **2020**, *9*, https://doi.org/10.3390/foods9050645.
8. Peng, X.-M.; LV Damu, G.; Zhou, H. Current developments of coumarin compounds in medicinal chemistry. *Current pharmaceutical design* **2013**, *19*, 3884-3930, https://doi.org/10.2174/1381612811319210013.
9. Sadeghi-Kaji, S.; Shareghi, B.; Saboury, A.A.; Farhadian, S. Spectroscopic and molecular docking studies on the interaction between spermidine and pancreatic elastase. *International journal of biological macromolecules* **2019**, *131*, 473-483, https://doi.org/10.1016/j.ijbiomac.2019.03.084.
10. Thakur, A.; Singla, R.; Jaitak, V. Coumarins as anticancer agents: a review on synthetic strategies, mechanism of action and SAR studies. *Eur J Med Chem* **2015**, *101*, 476-495, https://doi.org/10.1016/j.ejmech.2015.07.010.
11. Slivka, M.V.; Korol, N.I.; Fizer, M.M. Fused bicyclic 1, 2, 4-triazoles with one extra sulfur atom: Synthesis, properties, and biological activity. *Journal of Heterocyclic Chemistry* **2020**, *57*, 3236-3254, https://doi.org/10.1002/jhet.4044.
12. Agisho, H.A.; Esatu, H.; Hairat, S.; Zaki, M. TBHP/TBAI–Mediated simple and efficient synthesis of 3, 5-disubstituted and 1, 3, 5-trisubstituted 1H-1, 2, 4-triazoles via oxidative decarbonylation of aromatic aldehydes and testing for antibacterial activities. *Tetrahedron Letters* **2020**, *61*, https://doi.org/10.1016/j.tetlet.2020.151989.

13. Ghanaat, J.; A Khalilzadeh, M.; Zareyee, D. KF/CP NPs as an efficient nanocatalyst for the synthesis of 1, 2, 4-triazoles: Study of antioxidant and antimicrobial activity. *Eurasian Chemical Communications* **2020**, *2*, 202-212, https://dx.doi.org/10.33945/SAMI/ECC.2020.2.6.
14. Kocyigit-Kaymakcioglu, B.; Celen, A.O.; Tabanca, N.; Ali, A.; Khan, S.I.; Khan, I.A.; Wedge, D.E. Synthesis and biological activity of substituted urea and thiourea derivatives containing 1, 2, 4-triazole moieties. *Molecules* **2013**, *18*, 3562-3576, https://doi.org/10.3390/molecules18033562.
15. Shalini, K.; Kumar, N.; Drabu, S.; Sharma, P.K. Advances in synthetic approach to and antifungal activity of triazoles. *Beilstein journal of organic chemistry* **2011**, *7*, 668-677, https://dx.doi.org/10.3762%2Fbjoc.7.79.
16. Boraei, A.T.; Singh, P.K.; Sechi, M.; Satta, S. Discovery of novel functionalized 1, 2, 4-triazoles as PARP-1 inhibitors in breast cancer: Design, synthesis and antitumor activity evaluation. *European journal of medicinal chemistry* **2019**, *182*, https://doi.org/10.1016/j.ejmech.2019.111621.
17. Singh, R.; Kashaw, S.; Mishra, V.; Mishra, M.; Rajoriya, V.; Kashaw, V. Design and synthesis of new bioactive 1, 2, 4-Triazoles, potential antitubercular and antimicrobial agents. *Indian journal of pharmaceutical sciences* **2018**, *80*, 36-45, https://doi.org/10.4172/pharmaceutical-sciences.1000328.
18. Gupta, A.K.; Prachand, S.; Patel, A.; Jain, S. Synthesis of some 4-amino-5-(substituted-phenyl)-4H-[1, 2, 4] triazole-3-thiol derivatives and antifungal activity. *Int. J. Pharm. Life Sci* **2012**, *3*, 1848-1857.
19. Dawood, K.M.; Farag, A.M.; Abdel-Aziz, H.A. Synthesis and antimicrobial evaluation of some 1, 2, 4-triazole, 1, 3, 4-oxa (thia) diazole, and 1, 2, 4-triazolo [3, 4-b]-1, 3, 4-thiadiazine derivatives. *Heteroatom Chemistry: An International Journal of Main Group Elements* **2005**, *16*, 621-627.
20. Cardoso, C.S.; Silva, D.P.; Silva, D.M.; Florentino, I.F.; Fajemiroye, J.O.; Moreira, L.K.; Vasconcelos, J.P.; Sanz, G.; Vaz, B.G.; Lião, L.M. Mechanisms involved in the antinociceptive and anti-inflammatory effects of a new triazole derivative: 5-[1-(4-fluorophenyl)-1 H-1, 2, 3-triazol-4-yl]-1 H-tetrazole (LQFM-096). *Inflammopharmacology* **2020**, 1-16, https://doi.org/10.1007/s10787-020-00685-8.
21. Aswathanarayanappa, C.; Bheemappa, E.; Bodke, Y.D.; Krishnegowda, P.S.; Venkata, S.P.; Ningegowda, R. Synthesis and Evaluation of Antioxidant Properties of Novel 1, 2, 4-T riazole-Based Schiff Base Heterocycles. *Archiv der Pharmazie* **2013**, *346*, 922-930, https://doi.org/10.1002/ardp.201300202.
22. Khan, I.; Ali, S.; Hameed, S.; Rama, N.H.; Hussain, M.T.; Wadood, A.; Uddin, R.; Ul-Haq, Z.; Khan, A.; Ali, S. Synthesis, antioxidant activities and urease inhibition of some new 1, 2, 4-triazole and 1, 3, 4-thiadiazole derivatives. *European journal of medicinal chemistry* **2010**, *45*, 5200-5207, https://doi.org/10.1016/j.ejmech.2010.08.034.
23. Siddiqui, N.; Alam, M.; Ahsan, W. Synthesis, anticonvulsant and toxicity evaluation of 2-(1H-indol-3-yl) acetyl-N-(substituted phenyl) hydrazine carbothioamides and their related heterocyclic derivatives. *Acta Pharmaceutica* **2008**, *58*, 445-454, https://doi.org/10.2478/v10007-008-0025-0.
24. Küçükgüzel, I.; Küçükgüzel, S.G.; Rollas, S.; Kiraz, M. Some 3-thioxo/alkylthio-1, 2, 4-triazoles with a substituted thiourea moiety as possible antimycobacterials. *Bioorganic & medicinal chemistry letters* **2001**, *11*, 1703-1707, https://doi.org/10.1016/s0960-894x(01)00283-9.
25. Palaska, E.; Şahin, G.; Kelicen, P.; Durlu, N.T.; Altinok, G. Synthesis and anti-inflammatory activity of 1-acylthiosemicarbazides, 1, 3, 4-oxadiazoles, 1, 3, 4-thiadiazoles and 1, 2, 4-triazole-3-thiones. *Il Farmaco* **2002**, *57*, 101-107, https://doi.org/10.1016/S0014-827X(01)01176-4.
26. De Proft, F.; Geerlings, P. Conceptual and computational DFT in the study of aromaticity. *Chemical reviews* **2001**, *101*, 1451-1464, https://doi.org/10.1021/cr9903205.
27. Badry, R.; El-Khodary, S.; Elhaes, H.; Nada, N.; Ibrahim, M. On the molecular modeling analyses of sodium carboxymethyl cellulose treated with acetic acid. *Letters in Applied NanoBioScience* **2019**, *8*, 553-557, https://doi.org/10.33263/LIANBS82.553557.
28. Orek, C.; Koparir, P.; Koparir, M. N-cyclohexyl-2-[5-(4-pyridyl)-4-(p-tolyl)-4H-1, 2, 4-triazol-3-ylsulfanyl]-acetamide dihydrate: Synthesis, experimental, theoretical characterization and biological activities. *Spectrochimica Acta Part A: Molecular and Biomolecular Spectroscopy* **2012**, *97*, 923-934, https://doi.org/10.1016/j.saa.2012.07.082.
29. Cansız, A.; Cetin, A.; Orek, C.; Karatepe, M.; Sarac, K.; Kus, A.; Koparir, P. 6-Phenyl-3-(4-pyridyl)-1, 2, 4-triazolo-[3, 4-b][1, 3, 4] thiadiazole: Synthesis, experimental, theoretical characterization and biological activities. *Spectrochimica Acta Part A: Molecular and Biomolecular Spectroscopy* **2012**, *97*, 606-615, https://doi.org/10.1016/j.saa.2012.07.016.
30. Koparir, M.; Orek, C.; Alayunt, N.; Parlak, A.E.; Koparir, P.; Sarac, K.; Dastan, S.D.; Cankaya, N. Synthesis, Structure Investigation, Spectral Characteristics and Biological Activitie of 4-Benzyl-3-(2-Hydroxyphenyl)-1H-1, 2, 4-Triazole-5 (4H)-Thione. *Communications in Computational Chemistry* **2013**, *1*, 244-268, https://doi.org/10.4208/cicc.2013.v1.n3.5.
31. Loukhovitski, B.I.; Torokhov, S.A.; Loukhovitskaya, E.E.; Sharipov, A.S. DFT study of small aluminum and boron hydrides: isomeric composition and physical properties. *Structural Chemistry* **2018**, *29*, 49-68, https://doi.org/10.1007/s11224-017-1000-5.
32. Bayoumy, A.; Youssif, G.; Elgohary, E.; Husien, S.; Salah El Deen, H.; Albeltagy, N.; Abdelnaby, D.; Medhat, A.; Elhaes, H.; Ibrahim, M. Impact of solvation on the geometrical parameters of some amino acids. *Letters in Applied NanoBioScience* **2019**, *8*, 567-570.

33. Khalid, M.; Ullah, M.A.; Adeel, M.; Khan, M.U.; Tahir, M.N.; Braga, A.A.C. Synthesis, crystal structure analysis, spectral IR, UV–Vis, NMR assessments, electronic and nonlinear optical properties of potent quinoline based derivatives: interplay of experimental and DFT study. *Journal of Saudi Chemical Society* **2019**, *23*, 546-560, https://doi.org/10.1016/j.jscs.2018.09.006.
34. Oueslati, Y.; Kansız, S.; Valkonen, A.; Sahbani, T.; Dege, N.; Smirani, W. Synthesis, crystal structure, DFT calculations, Hirshfeld surface, vibrational and optical properties of a novel hybrid non-centrosymmetric material (C10H15N2) 2H2P2O7. *Journal of Molecular Structure* **2019**, *1196*, 499-507, https://doi.org/10.1016/j.molstruc.2019.06.110.
35. Adole, V.A.; Waghchaure, R.H.; Pathade, S.S.; Patil, M.R.; Pawar, T.B.; Jagdale, B.S. Solvent-free grindstone synthesis of four new (E)-7-(arylidene)-indanones and their structural, spectroscopic and quantum chemical study: a comprehensive theoretical and experimental exploration. *Molecular Simulation* **2020**, *46*, 1045-1054, https://doi.org/10.1080/08927022.2020.1800690.
36. Anzian, A.; Muhialdin, B.J.; Mohammed, N.K.; Kadum, H.; Marzlan, A.A.; Sukor, R.; Meor Hussin, A.S. Antibacterial activity and metabolomics profiling of torch ginger (Etlingera elatior Jack) flower oil extracted using subcritical carbon dioxide (CO2). *Evidence-Based Complementary and Alternative Medicine* **2020**, *2020*, https://doi.org/10.1155/2020/4373401.
37. Veloso, D.J.; Abrão, F.; Martins, C.H.; Bronzato, J.D.; Gomes, B.P.; Higino, J.S.; Sampaio, F.C. Potential antibacterial and anti-halitosis activity of medicinal plants against oral bacteria. *Archives of oral biology* **2020**, *110*, https://doi.org/10.1016/j.archoralbio.2019.104585.
38. Ağagündüz, D. Determination of the total antioxidant and oxidant status of some galactagogue and herbal teas. *Food Science and Human Wellness* **2020**, *9*, 377-382, https://doi.org/10.1016/j.fshw.2020.06.002.
39. Özcan, S.; Balci, M. The chemistry of homophthalic acid: a new synthetic strategy for construction of substituted isocoumarin and indole skeletons. *Tetrahedron* **2008**, *64*, 5531-5540, https://doi.org/10.1016/j.tet.2008.03.097.
40. Lin-Vien, D.; Colthup, N.B.; Fateley, W.G.; Grasselli, J.G. *The handbook of infrared and Raman characteristic frequencies of organic molecules*. Elsevier: **1991.**
41. Asemani, M.; Rabbani, A.R. Detailed FTIR spectroscopy characterization of crude oil extracted asphaltenes: Curve resolve of overlapping bands. *Journal of Petroleum Science and Engineering* **2020**, *185*, https://doi.org/10.1016/j.petrol.2019.106618.
42. Tammer, M.; Sokrates, G. *Infrared and Raman characteristic group frequencies: tables and charts*. Springer: **2004.**
43. Wilcock, P.; Piotrowski, C.; Haberl, B.; Smith, B.; Gahkani, A. Evaluation of Using Hand Held Near Infrared Spectroscopy for Pellet Fines and Moisture. *Journal of Animal Science* **2018**, *96*, 60-60, https://doi.org/10.1093/jas/sky073.112.
44. Thai, C.H.; Ferreira, A.; Phung-Van, P. A nonlocal strain gradient isogeometric model for free vibration and bending analyses of functionally graded plates. *Composite Structures* **2020**, *251*, https://doi.org/10.1016/j.compstruct.2020.112634.
45. Sarıkaya, E.K.; Dereli, Ö.; Erdoğdu, Y.; Güllüoğlu, M. Molecular structure and vibrational spectra of 7-Ethoxycoumarin by density functional method. *J Mol Struct* **2013**, *1049*, 220-226, https://doi.org/10.1016/j.molstruc.2013.06.026.
46. Okuno, M.; Yamada, S.; Ohto, T.; Tada, H.; Nakanishi, W.; Ariga, K.; Ishibashi, T.-A. Hydrogen Bonds and Molecular Orientations of Supramolecular Structure between Barbituric Acid and Melamine Derivative at the Air/Water Interface Revealed by Heterodyne-Detected Vibrational Sum Frequency Generation Spectroscopy. *The journal of physical chemistry letters* **2020**, *11*, 2422-2429, https://doi.org/10.1021/acs.jpclett.0c00329.
47. Sajan, D.; Erdogdu, Y.; Reshmy, R.; Dereli, Ö.; Kurien Thomas, K.; Hubert Joe, I. DFT-based molecular modeling, NBO analysis and vibrational spectroscopic study of 3-(bromoacetyl)coumarin. *Spectrochimica Acta Part A: Molecular and Biomolecular Spectroscopy* **2011**, *82*, 118-125, https://doi.org/10.1016/j.saa.2011.07.013.
48. Ahmed, L.; Rebaz, O. Spectroscopic properties of Vitamin C: A theoretical work. *Cumhuriyet Science Journal* **2020**, *41*, 916-928, http://dx.doi.org/10.17776/csj.762184.
49. Omer, R.A.; Ahmed, L.O.; Koparir, M.; Koparir, P. Theoretical analysis of the reactivity of chloroquine and hydroxychloroquine. *Indian Journal of Chemistry-Section A (IJCA)* **2020**, *59*, 1828-1834.
50. Rebaz, O.; Koparir, P.; Ahmed, L.; Koparir, M. Computational determination the reactivity of salbutamol and propranolol drugs. *Turkish Computational and Theoretical Chemistry* **2020**, *4*, 67-75.
51. Choudhary, V.; Bhatt, A.; Dash, D.; Sharma, N. DFT calculations on molecular structures, HOMO–LUMO study, reactivity descriptors and spectral analyses of newly synthesized diorganotin (IV) 2-chloridophenylacetohydroxamate complexes. *Journal of computational chemistry* **2019**, *40*, 2354-2363, https://doi.org/10.1002/jcc.26012.
52. Babaei, S.; Niad, M. Chemical reactivity descriptors as a tool of prediction in the synthesis of sandwich type polyoxometalate organic–inorganic hybrid compounds. *Polyhedron* **2020**, *188*, https://doi.org/10.1016/j.poly.2020.114710.

53. Madkour, L.H.; Kaya, S.; Guo, L.; Kaya, C. Quantum chemical calculations, molecular dynamic (MD) simulations and experimental studies of using some azo dyes as corrosion inhibitors for iron. Part 2: bis–azo dye derivatives. *Journal of Molecular Structure* **2018**, *1163*, 397-417, https://doi.org/10.1016/j.molstruc.2018.03.013.
54. Van, D.; Dinda, G.; Park, J.; Mazumder, J.; Lee, S.H. Enhancing hardness of Inconel 718 deposits using the aging effects of cold metal transfer-based additive manufacturing. *Materials Science and Engineering: A* **2020**, *776*, https://doi.org/10.1016/j.msea.2020.139005.
55. Zandiyeh, Z.; Ghiasi, R. A Theoretical Approach towards Identification of External Electric Field Effect on (η 5-C 5 H 5) Me 2 Ta (η 2-C 6 H 4). *Russian Journal of Physical Chemistry A* **2019**, *93*, 482-487, https://doi.org/10.1134/S0036024419030294.
56. Bayoumy, A.M.; Ibrahim, M.; Omar, A. Mapping molecular electrostatic potential (MESP) for fulleropyrrolidine and its derivatives. *Optical and Quantum Electronics* **2020**, *52*, 1-13, https://doi.org/10.1007/s11082-020-02467-6.
57. Politzer, P.; Murray, J.S. The fundamental nature and role of the electrostatic potential in atoms and molecules. *Theoretical Chemistry Accounts* **2002**, *108*, 134-142, https://doi.org/10.1007/s00214-002-0363-9.
58. Chattopadhyay, B.; Basu, S.; Chakraborty, P.; Choudhuri, S.K.; Mukherjee, A.K.; Mukherjee, M. Synthesis, spectroscopic characterization, X-ray powder structure analysis, DFT study and in vitro anticancer activity of N-(2-methoxyphenyl)-3-methoxysalicylaldimine. *J Mol Struct* **2009**, *932*, 90-96, https://doi.org/10.1016/j.molstruc.2009.05.047.
59. Famuyide, I.M.; Aro, A.O.; Fasina, F.O.; Eloff, J.N.; McGaw, L.J. Antibacterial and antibiofilm activity of acetone leaf extracts of nine under-investigated south African Eugenia and Syzygium (Myrtaceae) species and their selectivity indices. *BMC complementary and alternative medicine* **2019**, *19*, 1-13, https://doi.org/10.1186/s12906-019-2547-z.
60. Della Pelle, F.; Scroccarello, A.; Sergi, M.; Mascini, M.; Del Carlo, M.; Compagnone, D. Simple and rapid silver nanoparticles based antioxidant capacity assays: Reactivity study for phenolic compounds. *Food chemistry* **2018**, *256*, 342-349, https://doi.org/10.1016/j.foodchem.2018.02.141.